Applied Physics Letters

Effects of active layer thickness and thermal annealing on polythiophene: Fullerene bulk heterojunction photovoltaic devices

Cite as: Appl. Phys. Lett. **97**, 053305 (2010); https://doi.org/10.1063/1.3474654
Submitted: 18 June 2010 • Accepted: 04 July 2010 • Published Online: 04 August 2010

Lichang Zeng, Ching W. Tang and Shaw H. Chen

Effects of active layer thickness and thermal annealing on polythiophene: Fullerene bulk heterojunction photovoltaic devices

Lichang Zeng,[1] Ching W. Tang,[1,a)] and Shaw H. Chen[1,2]
[1]*Department of Chemical Engineering, University of Rochester, Rochester, New York 14627, USA*
[2]*Laboratory for Laser Energetics, University of Rochester, Rochester, New York 14623, USA*

(Received 18 June 2010; accepted 4 July 2010; published online 4 August 2010)

The effect of thermal annealing on photovoltaic devices comprising poly(3-hexylthiophene):[6,6]-phenyl C_{61} butyric acid methyl ester (P3HT:PCBM) with thicknesses up to 1200 nm was investigated. Without thermal annealing, the efficiency of the as-prepared devices decreased with increasing active layer thickness, reflecting largely a reduction in the short-circuit current density and an inverse photocurrent spectral response. Thermal annealing of the full devices was found to substantially recover thick-film device efficiencies while reducing the thin-film device efficiencies. The profound variations in photovoltaic characteristics were interpreted in terms of vertical phase separation in the P3HT:PCBM blend film and Li^+ diffusion from the LiF/Al contact. © *2010 American Institute of Physics*. [doi:10.1063/1.3474654]

The power conversion efficiency of organic photovoltaic (OPV) devices has steadily improved over the last decade due in large part to continuous refinements in the device structures based on planar[1] or bulk[2] heterojunctions. Among the most studied OPV devices to date is the poly(3-hexylthiophene): [6,6]-phenyl C_{61} butyric acid methyl ester (P3HT:PCBM) bulk-heterojunction cell based on a donor-acceptor blend film produced by casting a solution of P3HT and PCBM. In order to achieve high efficiency in OPV devices, the solution-cast P3HT:PCBM films are often subjected to thermal[3,4] or solvent-vapor annealing[5,6] or both to produce a bicontinuous phase in the film and to induce formation of crystalline P3HT domain. Thermal annealing of devices completed with electrodes has also been used to improve the device performance.[5] The highest efficiency reported for P3HT:PCBM devices is about 4%–5%,[4,5] which is obtained for a P3HT:PCBM layer with a thickness in the range of 100–250 nm. Although a thicker layer is desirable for light absorption, thick-film P3HT:PCBM devices have been found to be generally less efficient than thin-film devices, and are therefore, seldom explored in detail.[7] Low carrier mobility[8] and chemical purity issues[9] are often cited as the reasons for the inefficiency associated with thick-film OPV devices in general. In this study we have examined systematically a series of P3HT:PCBM photovoltaic devices where the active layer thickness is varied from 130 to 1200 nm. We will show that the device efficiency is strongly dependent on the layer thickness and can be profoundly affected by thermal annealing of the full device.

The OPV devices employed for this study have the structure ITO/MoO_x(3 nm)/P3HT:PCBM(z nm)/LiF(0.8 nm)/Al(100 nm), where the active layer is a P3HT:PCBM blend at 1:1 mass ratio with thickness z varying from 130 to 1200 nm. The transparent front contact is glass/ITO/MoO_x, where MoO_x is used to improve the ITO contact,[10] and the back contact is LiF/Al which is commonly used as ohmic contact in OPV devices[11] as well as organic light emitting diodes.[12] The details of the device fabrication and measurement procedures were described in Ref. 13. Figure 1(a) shows the current density-voltage (J-V) curves for a series of OPV devices without thermal annealing. The corresponding photovoltaic performance parameters: power conversion efficiency (η), short-circuit current density (J_{SC}), open-circuit voltage (V_{OC}) and fill factor (FF) are listed in Table I. The notable features are: (1) regardless of the P3HT:PCBM layer thickness the photocurrent exhibits a relatively weak dependence on the reverse bias voltage, yielding a FF of about 0.62 for all devices; (2) as the film

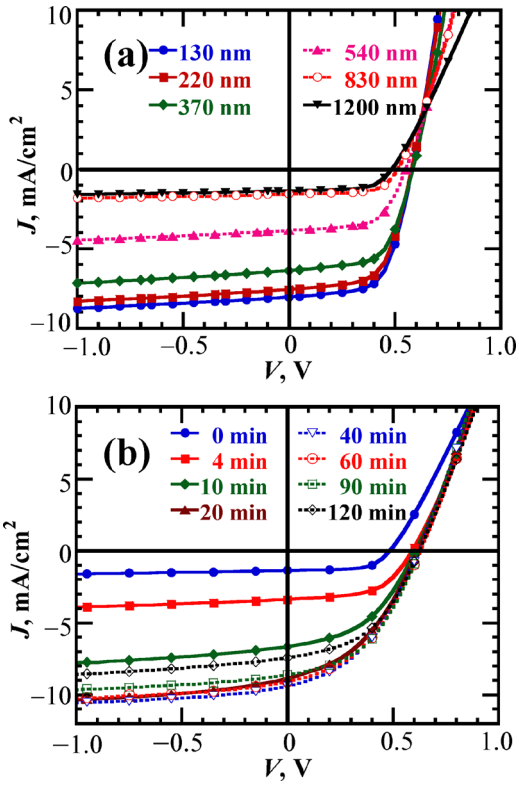

FIG. 1. (Color online) J-V characteristics under 100 mW/cm^2 white light illumination of (a) OPV devices with varying active layer thicknesses before thermal annealing, and (b) a 1200 nm OPV device thermally annealed at 110 °C up to 120 min.

a)Electronic mail: chtang@che.rochester.edu.

TABLE I. Performance parameters of OPV devices with varying active layer thicknesses before and after thermal annealing at 110 °C for 20 min.

	Unannealed				Annealed			
Thickness (nm)	J_{SC} (mA/cm^2)	V_{OC} (V)	FF	η (%)	J_{SC} (mA/cm^2)	V_{OC} (V)	FF	η (%)
130	8.2	0.58	0.61	2.9	4.4	0.57	0.42	1.1
220	7.6	0.58	0.61	2.7	5.3	0.60	0.54	1.7
370	6.4	0.58	0.62	2.3	6.7	0.61	0.57	2.4
540	3.9	0.55	0.61	1.3	8.7	0.61	0.53	2.8
830	1.6	0.52	0.65	0.5	11.3	0.61	0.45	3.1
1200	1.3	0.50	0.64	0.4	9.2	0.61	0.40	2.3

thickness increases from 130 to 1200 nm, the J_{SC} decreases sharply from 8.2 to 1.3 mA/cm^2 along with a modest decrease in V_{OC} from 0.58 to 0.50 V. The absorption spectra of the P3HT:PCBM films (Fig. S1 of Ref. 13) show a main peak at 515 nm with two shoulders at 560 and 610 nm, which are characteristic of crystalline P3HT.[4,5] The spectral responses are shown in Fig. 2(a) as plots of external quantum efficiency (collected charge per incident photon) as a function of wavelength. For the thin-film devices, the spectral response tracks approximately the P3HT:PCBM absorption spectrum with a maximum η_{EQE} of about 50% in the spectral range of 500 to 600 nm. As the P3HT:PCBM film thickness increases, the spectral response shows an increasingly inverse behavior with η_{EQE} descending to a minimum in the absorption region. For the thick-film devices (800–1200 nm), the maximum η_{EQE} is only about 10% and shifted toward the

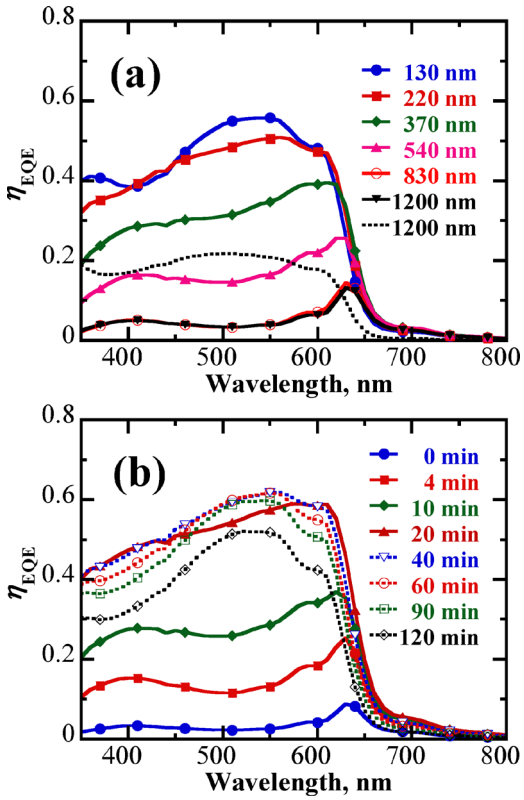

FIG. 2. (Color online) (a) Spectral responses of OPV devices with varying active layer thicknesses before thermal annealing; the dotted curve represents the spectral response from a 1200 nm device under illumination through the semitransparent back contact. (b) Spectral responses of a 1200 nm OPV device thermally annealed at 110 °C up to 120 min.

P3HT absorption edge at 630 nm, and the minimum η_{EQE} is below 5% at the absorption region of 500–600 nm. The highest η obtained without annealing is 2.9% for the 130 nm device, whereas the lowest η is 0.4% for the 1200 nm device.

The effect of thermal annealing is shown in Fig. 1(b), where the *J-V* curves are plotted for a thick-film device (1200 nm). This device was subjected to 110 °C annealing over a cumulative period of 2 h. It can be seen that significant improvements in OPV characteristics are obtained even with an annealing time as short as a few minutes. The J_{SC} increases steadily upon annealing, reaching a maximum value of 10.1 mA/cm^2 after 40 min, along with an increase in V_{OC} from 0.50 to 0.62 V. However, the FF is decreased from 0.64 to 0.40, yielding an overall increase in efficiency from 0.4% prior to annealing to 2.6% for a cumulative annealing of 90 min at 110 °C. Further annealing has resulted in deterioration of OPV device performance. As shown in Fig. S2 in Ref. 13, thermal annealing does not significantly alter the absorption spectrum of the P3HT:PCBM layer. In contrast, the spectral response of the OPV device is dramatically affected by thermal annealing, reverting from inverse to normal behavior upon increasing the annealing duration as shown in Fig. 2(b). In fact, η_{EQE} values as high as 60% are obtained around the absorption maximum region of 500–600 nm for this device after annealing for 90 min. The effects of thermal annealing on devices of various P3HT:PCBM layer thicknesses are summarized in Table I where the OPV parameters for the devices before and after annealing at 110 °C for 20 min are compared. It can be seen that whereas the efficiency of the thick-film devices (570–1200 nm) is significantly improved upon thermal annealing, the efficiency of the thin-film devices (130–220 nm) is adversely affected under the same annealing condition. In fact, thermal annealing has led to a steep drop in efficiency from 2.9% to 1.1% in the thinnest device (130 nm), reflecting a large decrease in J_{SC} from 8.2 to 4.4 mA/cm^2 and in FF from 0.61 to 0.42. For comparison, the efficiency drops from 2.7% to 1.7% for the 220 nm device and remains essentially unchanged at 2.3% for the thicker 370 nm device.

Qualitatively, the trend in OPV efficiency upon thermal annealing can be explained in terms of a graded-composition model and lithium diffusion from the back LiF/Al electrode. The graded-composition model is based on the phenomenon of vertical phase separation in which the P3HT and PCBM components in the blended film segregate spontaneously during deposition or induced by various postdeposition treatments, resulting in different photogeneration

efficiencies.[14–16] To explain the low efficiency of the thick-film devices prior to thermal annealing, we posit that P3HT:PCBM has a graded composition with a low-efficiency, presumably P3HT-rich, phase adjacent to the ITO/MoO_x surface and a high-efficiency, presumably PCBM-rich, phase on top. By acting essentially as a filter to block light penetration to the PCBM-rich phase, the P3HT-rich phase causes an inverse spectral response and a large reduction in efficiency. To confirm this explanation, a 1200 nm device was fabricated with a transparent Al (2 nm)/Ag(10 nm) in place of a thick Al (100 nm) as the back electrode. By illumination through this back electrode, a normal spectral response (shown in Fig. 2(a)) was obtained consistent with the absorption spectrum of P3HT as opposed to an inverse spectral response obtained with illumination through the front ITO/MoO_x electrode.

The recovery of efficiency along with the reversal of the spectral response from inverse to normal upon thermal annealing for the thick-film devices can be attributed to the thermally activated molecular diffusion of PCBM into the P3HT-rich bottom phase, forming crystalline PCBM domains, which in effect transforms the inefficient P3HT-rich phase to a more efficient phase with a balanced P3HT:PCBM composition. Such an effect has also been previously observed for C_{60} (Ref. 17) and PCBM (Ref. 18) in polymer/fullerene bilayer films with thermal annealing.

The effect of thermal annealing on the thin-film devices appears to contradict the graded composition model. The efficiency of the thin-film devices is relatively high prior to thermal annealing, indicating that the inefficient P3HT-rich phase, if present, is not thick enough to affect the device performance. In any case, it would be difficult to associate the degradation in efficiency in these devices upon thermal annealing with the presence or absence of such a layer. We note that the dark current has increased significantly with thermal annealing of the thin-film devices. As shown in Fig. S3 of Ref. 13, the log *J-V* plots reveal an excessively high reverse dark current density (~ 1 mA/cm^2 at -1 V) for the annealed 130 nm device with LiF/Al as the back electrode. In contrast, the annealed 130 nm device with only Al as the back electrode exhibits a dark current density that is lower by almost three orders of magnitude. These results indicate that the diffusion of Li^+ ion from the LiF/Al source and the possible formation of Li^+PCBM^- complexes in the P3HT:PCBM layer is responsible for the increased conductivity in the 130nm device.[19] Moreover, the presence of Li^+ throughout the thin P3HT:PCBM layer, which is detrimental to the photogeneration process, is also the likely cause for the degradation of efficiency upon thermal annealing of the thin-film devices. In the absence of Li^+, as in devices with only Al as the back electrode, the high efficiency can generally be retained or even improved in thin-film P3HT:PCBM devices with thermal annealing, as observed in this study and also reported by Ma *et al.*[4] For thick-film devices with LiF/Al electrode, the reverse leakage current remains relatively low, as shown in Fig. S3 of Ref. 13 for a 1200 nm device, indicating that Li^+ diffusion into the thick P3HT:PCBM layer is range or source limited and apparently does not cause significant loss in efficiency to offset the large gain from penetraction of PCBM domain due to thermal annealing.

In summary, bulk heterojunction P3HT:PCBM photovoltaic devices with a layer thickness up to 1200 nm were characterized with respect to thermal annealing of the full device structure. Without annealing, the short circuit current density and power conversion efficiency both decreased with increasing film thickness. Concomitantly, the spectral response revealed an increasing inverse behavior. Annealing at 110 °C was found to increase dramatically the efficiency of the thick-film devices while decrease that of the thin-film devices. These variations in device characteristics can be understood in terms of vertical phase separation in P3HT:PCBM films and Li^+ diffusion from the Al/LiF back contact.

S.H.C. acknowledges financial support by the Department of Energy Office of Inertial Confinement Fusion under Cooperative Agreement No. DE-FC52-08NA28302 and the New York State Energy Research and Development Authority through the Laborstory for Laser Energetics, University of Rochester. The support of DOE does not constitute an endorsement by DOE of the views expressed in this article.

[1] C. W. Tang, Appl. Phys. Lett. **48**, 183 (1986).
[2] G. Yu, J. Gao, J. C. Hummelen, F. Wudle, and A. J. Heeger, Science **270**, 1789 (1995).
[3] F. Padinger, R. Rittberger, and N. Sariciftci, Adv. Funct. Mater. **13**, 85 (2003).
[4] W. L. Ma, C. Y. Yang, X. Gong, K. Lee, and A. J. Heeger, Adv. Funct. Mater. **15**, 1617 (2005).
[5] G. Li, S. Shrotriya, J. S. Huang, Y. Yao, T. Moriarty, K. Emery, and Y. Yang, Nature Mater. **4**, 864 (2005).
[6] Y. Zhao, Z. Y. Xie, Y. Qu, Y. H. Geng, and L. X. Wang, Appl. Phys. Lett. **90**, 043504 (2007).
[7] M. S. Kim, B. G. Kim, and J. S. Kim, ACS Appl, Mater. Interfaces **1**, 1264 (2009).
[8] A. J. Moulé, J. B. Bonekamp, and K. Meerholz, J. Appl. Phys. **100**, 094503 (2006).
[9] K. Sakai and M. Hiramoto, Mol. Cryst. Liq. Cryst. **491**, 284 (2008).
[10] V. Shrotriya, G. Li, Y. Yao, C. W. Chu, and Y. Yang, Appl. Phys. Lett. **88**, 073508 (2006).
[11] E. Ahlswede, J. Hanisch, and M. Powalla, Appl. Phys. Lett. **90**, 163504 (2007).
[12] L. S. Hung, C. W. Tang, and M. G. Mason, Appl. Phys. Lett. **70**, 152 (1997).
[13] See supplementary material at http://dx.doi.org/10.1063/1.3474654 for OPV device fabrication and characterization.
[14] M. Campoy-Quiles, T. Ferenczi, T. Agostinelli, P. G. Etchegoin, Y. Kim, T. Anthopoulos, P. N. Stavrinou, D. D. C. Bradley, and J. Nelson, Nature Mater. **7**, 158 (2008).
[15] Z. Xu, L. M. Chen, G. W. Yang, C. H. Huang, J. H. Hou, Y. Wu, G. Li, C. S. Hsu, and Y. Yang, Adv. Funct. Mater. **19**, 1227 (2009).
[16] S. S. van Bavel, E. Sourty, G. de With, and J. Loos, Nano Lett. **9**, 507 (2009).
[17] M. Drees, R. M. Davis, and J. R. Heflin, Phys. Rev. B **69**, 165320 (2004).
[18] A. Kumar, G. Li, Z. R. Hong, and Y. Yang, Nanotechnology **20**, 165202 (2009).
[19] H. Tachikawa, J. Phys. Chem. C **111**, 13087 (2007).